pubs.acs.org/acschemicalbiology

Articles

Subtype-Selective Positive Modulation of $K_{Ca}2.3$ Channels Increases Cilia Length

Young-Woo Nam, Rajasekharreddy Pala, Naglaa Salem El-Sayed, Denisse Larin-Henriquez, Farideh Amirrad, Grace Yang, Mohammad Asikur Rahman, Razan Orfali, Myles Downey, Keykavous Parang, Surya M. Nauli,* and Miao Zhang*

Cite This: *ACS Chem. Biol.* 2022, 17, 2344–2354

Read Online

ACCESS | Metrics & More | Article Recommendations | Supporting Information

ABSTRACT: Small-conductance Ca^{2+}-activated potassium ($K_{Ca}2.x$) channels are gated exclusively by intracellular Ca^{2+}. The activation of $K_{Ca}2.3$ channels induces hyperpolarization, which augments Ca^{2+} signaling in endothelial cells. Cilia are specialized Ca^{2+} signaling compartments. Here, we identified compound **4** that potentiates human $K_{Ca}2.3$ channels selectively. The subtype selectivity of compound **4** for human $K_{Ca}2.3$ over rat $K_{Ca}2.2a$ channels relies on an isoleucine residue in the HA/HB helices. Positive modulation of $K_{Ca}2.3$ channels by compound **4** increased flow-induced Ca^{2+} signaling and cilia length, while negative modulation by AP14145 reduced flow-induced Ca^{2+} signaling and cilia length. These findings were corroborated by the increased cilia length due to the expression of Ca^{2+}-hypersensitive $K_{Ca}2.3$_G351D mutant channels and the reduced cilia length resulting from the expression of Ca^{2+}-hyposensitive $K_{Ca}2.3$_I438N channels. Collectively, we were able to associate functions of $K_{Ca}2.3$ channels and cilia, two crucial components in the flow-induced Ca^{2+} signaling of endothelial cells, with potential implications in vasodilation and ciliopathic hypertension.

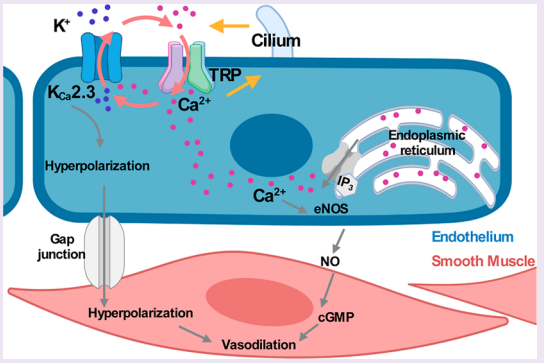

1. INTRODUCTION

Small- and intermediate-conductance Ca^{2+}-activated K^+ ($K_{Ca}2.x/K_{Ca}3.1$ or SK/IK) channels are activated exclusively by intracellular Ca^{2+}.[1,2] Four subtypes in the $K_{Ca}2.x/K_{Ca}3.1$ channel family are encoded by the *KCNN* mammalian genes: including *KCNN*1 for $K_{Ca}2.1$ (SK1), *KCNN*2 for $K_{Ca}2.2$ (SK2), *KCNN*3 for $K_{Ca}2.3$ (SK3), and *KCNN*4 for $K_{Ca}3.1$ (IK or SK4) channels.

In blood vessels, $K_{Ca}2.3$ and $K_{Ca}3.1$ channel subtypes are often detected on the plasma membrane of endothelial (ET) cells,[3−5] whereas $K_{Ca}2.1$ and $K_{Ca}2.2$ channel currents are rarely identifiable on the ET cell surface.[6] $K_{Ca}2.3$ and $K_{Ca}3.1$ channel subtypes seem to have a distinctive distribution and function in ET cells. $K_{Ca}3.1$ channels are often found on the ET cell membrane close to the endoplasmic reticulum (ER) Ca^{2+} store.[7−9] Ca^{2+} release from the ER triggered by acetylcholine or bradykinin receptors may lead to the opening of $K_{Ca}3.1$ channels nearby.[10] In contrast, $K_{Ca}2.3$ channels seem to co-localize with mechanosensitive or receptor-operated transient receptor potential (TRP) cation channels.[10,11] Ca^{2+} influx through these cation channels may activate $K_{Ca}2.3$ channels. The outflow of K^+ can hyperpolarize ET cells, increase the inward electrochemical gradient for Ca^{2+}, and augment the Ca^{2+} influx, which in turn enhances nitric oxide (NO) releases.[12,13]

Non-motile primary cilia are sensory organelles that sense fluid shear stress on the apical membrane of the cells.[14−16] Fluid flow that produces enough drag force on the top of the cells will bend and activate sensory cilia. Transgenic mouse models with cilia mutations do not survive at birth, confirming the importance of primary cilia in the physiological processes.[17−20] Primary cilia in vasculatures were once thought to be vestigial organelles and nonfunctional remnants. It has since been shown by different laboratories that cilia are mechanosensory organelles.[21−25] Cilia in ET cells sense changes in the fluid shear stress and trigger Ca^{2+} signaling and NO releases.[26,27]

Primary cilia have been known as specialized Ca^{2+} signaling compartments.[28,29] Ca^{2+} influx through TRPM4, TRPV4, TRPC1, polycystic kidney disease 2 (PKD2), and L-type voltage-gated Ca^{2+} (Ca_v) channels has been considered the main Ca^{2+} source for cilia.[28,29] Ca^{2+} influx in response to fluid shear stress activates ET $K_{Ca}2.3$ channels.[30] In ET cells, $K_{Ca}2.3$ channels functionally couple with Ca^{2+}-permeable PKD2[11] and

Received: May 28, 2022
Accepted: July 20, 2022
Published: August 10, 2022

https://doi.org/10.1021/acschembio.2c00469
ACS Chem. Biol. 2022, 17, 2344−2354

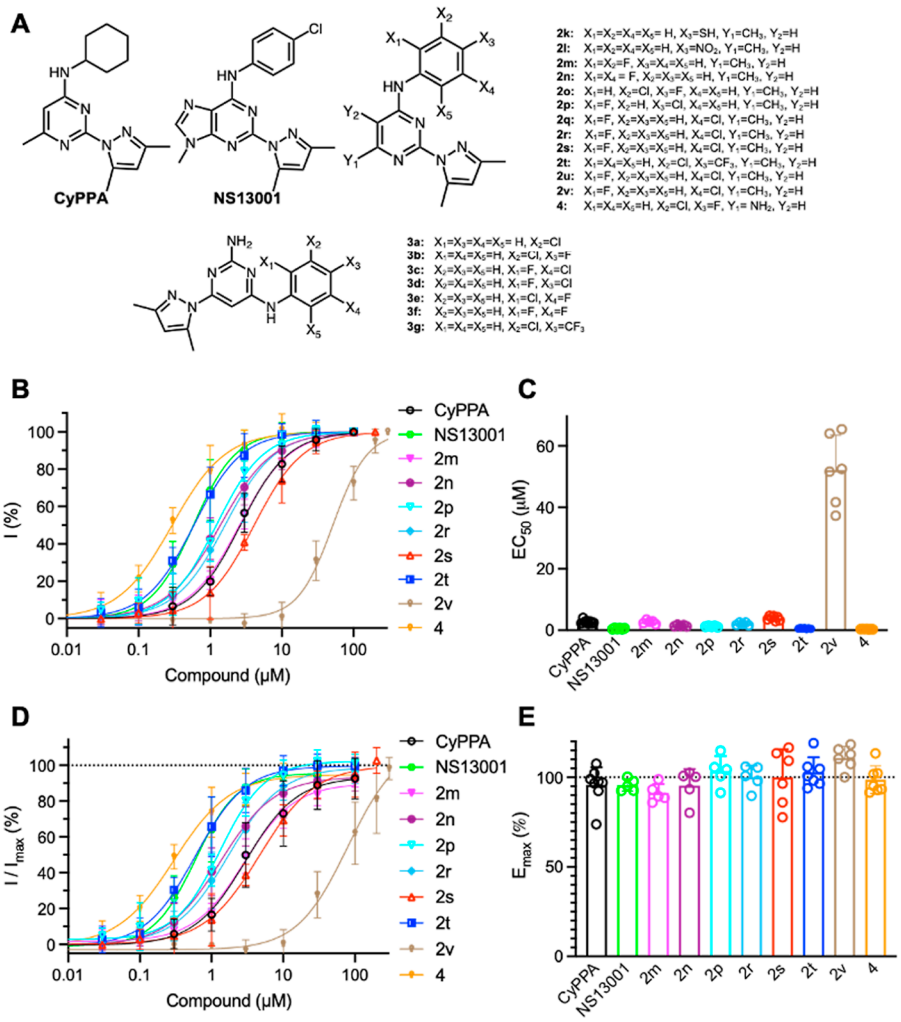

Figure 1. Positive modulation of human $K_{Ca}2.3$ channels by compounds. (A) Chemical structures of compounds **2k**−**2v**, **3a**−**3g**, and **4**, compared with those of CyPPA and NS13001. (B) Concentration-dependent potentiation of $K_{Ca}2.3$ channels by compounds. (C) EC_{50} values to compounds of $K_{Ca}2.3$ channels. (D) Responses to compounds of $K_{Ca}2.3$ channels were normalized to the maximal currents induced by 10 μM Ca^{2+}. (E) E_{max} to compounds of $K_{Ca}2.3$ channels. The numbers of independent recordings are shown in parentheses for CyPPA (8), NS13001 (5), **2m** (5), **2n** (5), **2p** (5), **2r** (5), **2s** (6), **2t** (7), **2v** (6), and **4** (7). Data are presented as mean ± SD.

TRPV4[31] channels and exert a positive feedback influence on intracellular Ca^{2+} signaling.[12,32] However, it is not clear whether this positive feedback mechanism extends back to the cilia, that is, whether the activation of $K_{Ca}2.3$ channels increases cilia length.

$K_{Ca}2.3$ and $K_{Ca}2.2a$ channels have similar amino acid sequences in their cytoplasmic gates, which makes it difficult to develop subtype-selective positive modulators discriminating these two subtypes. We recently identified the binding site of a prototype $K_{Ca}2.2a/K_{Ca}2.3$ channel modulator, CyPPA.[33] We have synthesized a new series of CyPPA analogues.[34] Here, we report the identification of a subtype-selective $K_{Ca}2.3$ channel modulator, compound **4**, that is ∼21-fold more potent on potentiating human $K_{Ca}2.3$ than rat $K_{Ca}2.2a$ channels. The subtype selectivity of compound **4** relies on an I-to-V amino acid residue difference between $K_{Ca}2.3$ and $K_{Ca}2.2a$ channels. The pharmacological activation of $K_{Ca}2.3$ channels by compound **4** increased cilia length, whereas the pharmacological inhibition of $K_{Ca}2.3$ channels by AP14145 decreased cilia length in a cultured ET cell line, suggesting the critical role of $K_{Ca}2.3$ channels in the regulation of cilia.

2. RESULTS

2.1. Compound 4 Subtype Selectively Modulates $K_{Ca}2.3$ Channels. A series of CyPPA analogues (Figure 1A) were synthesized as described in our previous report.[34] The potency of these compounds was measured using inside-out patch clamp electrophysiology recordings with human $K_{Ca}2.3$ channels heterologously expressed in HEK293 cells. Positive modulators of $K_{Ca}2$ channels require minimal concentration of Ca^{2+} to be effective.[35] Therefore, we measured the concentration-dependent responses of the channels to compounds in the presence of 0.15 μM Ca^{2+} (Figure S1). To construct the concentration−response curves, the current amplitudes at −90 mV in response to various concentrations of the compound were normalized to that obtained at the maximal concentration of the compound. The normalized currents were plotted as a function of the compound concentrations. CyPPA, NS13001, and our compounds **2m**−**2n**, **2p**, **2r**−**2t**, **2v**, and **4** concentration-dependently potentiated the activity of $K_{Ca}2.3$ channels (Figure 1B). Among them, NS13001 and compounds **2t** and **4** exhibited submicromolar EC_{50} values (Figure 1C).

https://doi.org/10.1021/acschembio.2c00469
ACS Chem. Biol. 2022, 17, 2344−2354

The responses induced by 10 μM Ca^{2+} are considered the maximal currents of the $K_{Ca}2.x$ channels.[35] To evaluate the efficacy (E_{max}) of the compounds on $K_{Ca}2.3$ channels, the current amplitudes at −90 mV in response to the compounds were normalized to that obtained at 10 μM Ca^{2+} [I/I_{max}(%), Figure 1D]. Non-linear regression curve fitting yielded E_{max} values for compounds on $K_{Ca}2.3$ channels that are comparable to the E_{max} of CyPPA (96 ± 10%, n = 8, Figure 1E).

The potency of these compounds on potentiating human $K_{Ca}2.3$ channels is summarized in Table 1 and compared with their previously determined EC_{50} values on rat $K_{Ca}2.2a$ channels.[34] CyPPA and NS13001 exhibited ∼2.7- and ∼4.3-fold selectivity for human $K_{Ca}2.3$ channels over rat $K_{Ca}2.2a$ channels (Table 1). Compounds **2t** and **4** are ∼6.3 and ∼21 times more potent, respectively, on potentiating the activity of human $K_{Ca}2.3$ channels than that of rat $K_{Ca}2.2a$ channels (Table 1). Among these compounds, compound **4** caught our attention with its ∼21-fold selectivity for human $K_{Ca}2.3$ channels over that of rat $K_{Ca}2.2a$ channels (Table 1). We further evaluated the effects of compound **4** on $K_{Ca}2.1$ and $K_{Ca}3.1$ channel subtypes. Compound **4** did not potentiate human $K_{Ca}2.1$ and human $K_{Ca}3.1$ channel subtypes substantively (Figure S2).

Table 1. Potency of Compounds on Human $K_{Ca}2.3$ Channels Compared with That on Rat $K_{Ca}2.2a$ Channels[a]

compound	EC_{50} on rat $K_{Ca}2.2a$ (mean ± SD, μM)	EC_{50} on human $K_{Ca}2.3$ (mean ± SD, μM)
CyPPA	7.5 ± 1.6[34]	2.7 ± 0.6
NS13001	2.2 ± 0.5[34]	0.50 ± 0.18
2k	>100[34]	>100
2l	>100[34]	>100
2m	5.0 ± 1.1[34]	2.7 ± 0.6
2n	1.9 ± 0.4[34]	1.5 ± 0.3
2o	1.0 ± 0.2[34]	0.20 ± 0.07[34]
2p	2.0 ± 0.3[34]	1.2 ± 0.2
2q	0.64 ± 0.12[34]	0.60 ± 0.10[34]
2r	3.0 ± 0.7[34]	2.1 ± 0.4
2s	3.5 ± 1.0[34]	3.9 ± 0.7
2t	3.3 ± 0.8[34]	0.52 ± 0.09
2u	>100[34]	>100
2v	>30[34]	52 ± 11
3a	>100[34]	>100
3b	>100[34]	>100
3c	>100[34]	>100
3d	>100[34]	>100
3e	>100[34]	>100
3f	>100[34]	>00
3g	>100[34]	>100
4	6.7 ± 1.6[34]	0.31 ± 0.07

[a]Some EC_{50} values are reported in ref 34.

2.2. Subtype Selectivity of Compound 4 Relies on the HA/HB Helices. Our recent study has revealed that the subtype selectivity of CyPPA for $K_{Ca}2.2a$ and $K_{Ca}2.3$ over $K_{Ca}3.1$ channels relies on the HA/HB helices.[33] We aligned the amino acid sequences of the rat $K_{Ca}2.2a$, human $K_{Ca}2.3$, and human $K_{Ca}3.1$ channel subtypes in the proximal C terminus (Figure 2A). Rat $K_{Ca}2.2a$ has a valine residue (V420) equivalent to a methionine residue (M311) of the human $K_{Ca}3.1$ channel in the HA helix. In the HB helix, rat $K_{Ca}2.2a$ has a lysine residue (K467), corresponding to an arginine residue (R355) of the human $K_{Ca}3.1$ channel. The V-to-M and K-to-R discrepancies between the amino acid sequences of rat $K_{Ca}2.2a$ and human $K_{Ca}3.1$ channels provide an explanation for the subtype selectivity of CyPPA.[33]

We then set out to explore the structural determinants for the ∼21-fold subtype selectivity of compound **4** for human $K_{Ca}2.3$ over rat $K_{Ca}2.2$ channels. Human $K_{Ca}2.3$ has an isoleucine (I568) equivalent to V420 in the HA helix of rat $K_{Ca}2.2a$ channels (Figure 2A). The side chain of $K_{Ca}2.3$_I568 would be bulkier than that of $K_{Ca}2.2a$_V420. Thus, the different sizes of a valine (rat $K_{Ca}2.2a$_V420) and an isoleucine (human $K_{Ca}2.3$_I568) may constitute the structural determinants for the subtype selectivity of compound **4**. We tested this hypothesis by mutating $K_{Ca}2.3$_I568 to its corresponding amino acid residue in $K_{Ca}2.2a$, a valine (Figure 2B). The $K_{Ca}2.3$_I568V mutant channel exhibited an EC_{50} value of 6.2 ± 1.3 μM (n = 6), which is ∼20-fold less sensitive to compound **4** than the $K_{Ca}2.3$_WT with an EC_{50} value of 0.31 ± 0.07 μM (n = 7, Figure 2C). The $K_{Ca}2.3$_I568V mutation did not affect the E_{max} values to compound **4**, compared with the $K_{Ca}2.3$_WT channel (Figure 2D,E). The $K_{Ca}2.3$_I568V mutation did not influence the apparent Ca^{2+} sensitivity of $K_{Ca}2.3$ channels (Figure S3A,B).

The corresponding mutation in rat $K_{Ca}2.2a$ channels ($K_{Ca}2.2a$_V420I) did not change either the apparent Ca^{2+} sensitivity of $K_{Ca}2.2a$ channels (Figure S4A,B) or the E_{max} to compound **4** (Figure S4C,D). The $K_{Ca}2.2a$_V420I increased the sensitivity of the channel to compound **4** (Figure S4E,F), corroborating the results acquired from the corresponding $K_{Ca}2.3$_I568V mutation (Figure 2B,C).

2.3. Pharmacological Modulation of $K_{Ca}2.3$ Channels Affected Cilia Length. Recently, we identified $K_{Ca}2.3$ channels as the predominant subtype expressed in a mouse ET cell line, whereas the expression of $K_{Ca}2.1$, $K_{Ca}2.2$, and $K_{Ca}3.1$ channel subtypes was not detected by immunoblots.[36] Thus, we examined whether negative modulation by AP14145 of $K_{Ca}2.3$ channels affected the cilia length of the ET cells. AP14145 inhibited $K_{Ca}2.3$ channels with an IC_{50} value of 0.97 ± 0.39 μM (n = 5, Figure S5).

ET cells were incubated with AP14145 (20 μM) for 2 days before cells reached confluency, and the cilia length was evaluated using immunostaining with the antibody of the ciliary marker acetylated α-tubulin (green) and the nuclear marker DAPI (blue, Figure S6A). AP14145 shortened cilia to 2.8 ± 0.1 μm, compared with 6.3 ± 0.3 μm of the solvent control group (Figure S6B,C), suggesting a regulatory role of $K_{Ca}2.3$ channels in the cilia length of ET cells.

Compound **4** potentiated $K_{Ca}2.3$ channels with an EC_{50} value of 0.31 ± 0.07 μM (n = 7) (Table 1 and Figure 1C). ET cells were incubated with compound **4** (20 μM) for 2 days before cells reached confluency, and the cilia length was evaluated using immunostaining with the antibody of the ciliary marker acetylated α-tubulin (green) and the nuclear marker DAPI (blue, Figure 3A). Compound **4** increased the cilia length to 6.1 ± 0.6 μm compared with 4.3 ± 0.3 μm of the solvent control group (Figure 3B,C), suggesting potential therapeutic usefulness of $K_{Ca}2.3$ channel positive modulators (e.g., compound **4**) in ciliopathy disease states with abnormal cilia.

To confirm the elongating effect of compound **4** on cilia (Figure 3), an additional ciliary marker Arl13b was used to measure the cilia length (Figure S7A). Also, the γ-tubulin was used as a marker for the basal body (base of a cilium), which

https://doi.org/10.1021/acschembio.2c00469
ACS Chem. Biol. 2022, 17, 2344−2354

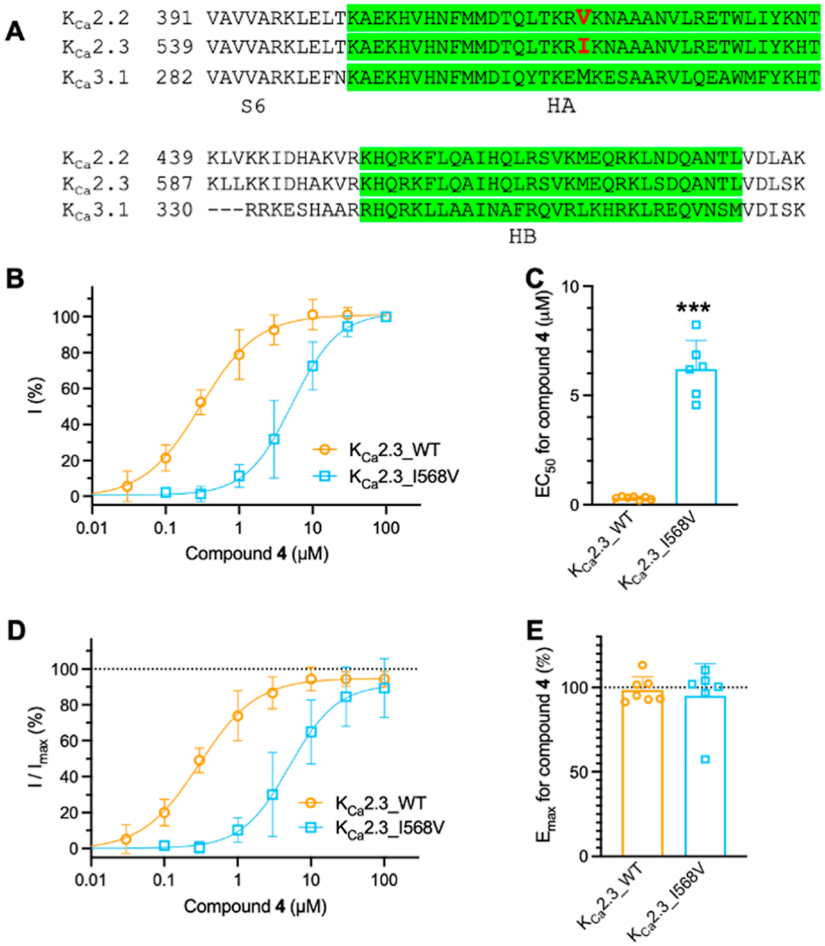

Figure 2. Subtype selectivity of compound 4 relies on the HA/HB helices. (A) Amino acid sequence alignment of rat $K_{Ca}2.2a$ [GenBank: NP_062187.1], human $K_{Ca}2.3$ [GenBank: NP_002240.3], and human $K_{Ca}3.1$ [GenBank: NP_002241.1] channels at the proximal C terminus. HA and HB helices are highlighted in green. I568 in $K_{Ca}2.3$ channels and their equivalent residues are shown in bold. (B) Potentiation by compound **4** of the WT and mutant human $K_{Ca}2.3$ channels. (C) EC_{50} values for potentiation by compound **4**. ***$P < 0.001$ compared with human $K_{Ca}2.3$_WT. (D) Responses to compound **4** were normalized to the maximal currents induced by 10 μM Ca^{2+}. (E) E_{max} to compound **4** of the WT and mutant $K_{Ca}2.3$ channels. The numbers of independent recordings are shown in parentheses for $K_{Ca}2.3$_WT (7) and $K_{Ca}2.3$_I568V (6). Data are presented as mean ± SD.

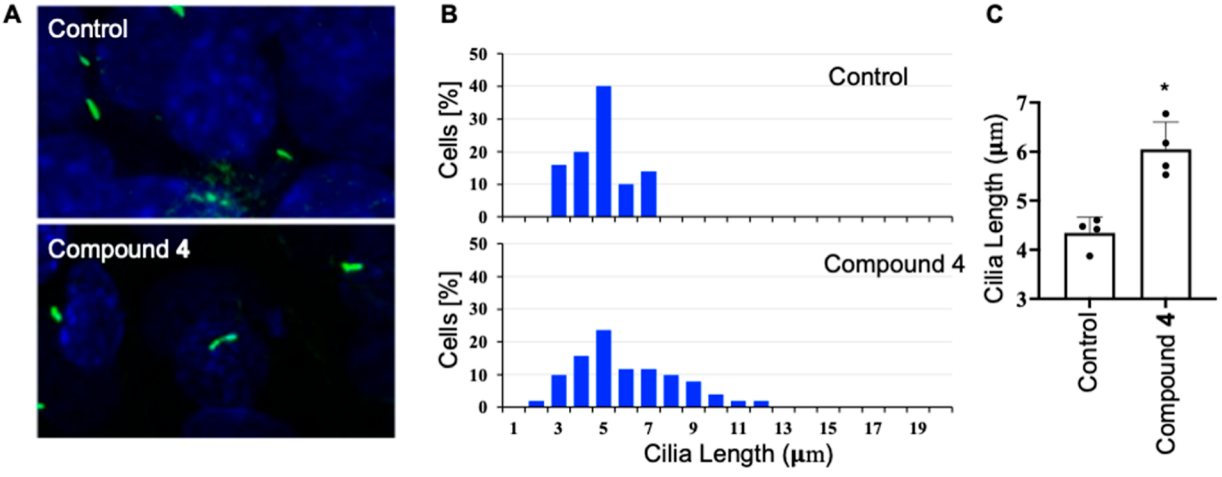

Figure 3. The effects of $K_{Ca}2.3$ channel potentiation by compound 4 on cilia length in ET cells. (A) Cells were stained with the antibody of the ciliary marker acetylated α-tubulin (green) and the nuclear marker (DAPI; blue). (B) Cilia length was grouped in a discreet range, and percent distribution was tabulated. (C) Cilia length is significantly longer in cells treated with the positive modulator, compound **4** (20 μM). $N = 50–70$ for each slide preparation, and a total of four independent slides were used in each group. Data are presented as mean ± SD. *$p < 0.05$ compared to the control.

https://doi.org/10.1021/acschembio.2c00469
ACS Chem. Biol. 2022, 17, 2344−2354

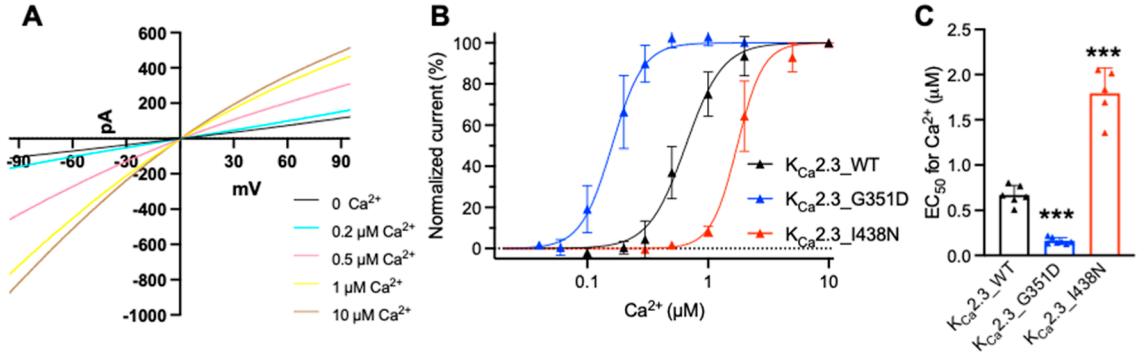

Figure 4. Mutant mouse $K_{Ca}2.3$ channels with altered Ca^{2+} sensitivity. Mutations channels were expressed in ET cells and their apparent Ca^{2+} sensitivity was evaluated using inside-out patch clamp recordings. (A) Representative $K_{Ca}2.3$_WT channel currents in response to Ca^{2+}. (B) Concentration-dependent activation by Ca^{2+} of the mutant and WT $K_{Ca}2.3$ channels. (C) EC_{50} values to Ca^{2+} of the mutant and WT $K_{Ca}2.3$ channels. The numbers of independent recordings are shown in parentheses for $K_{Ca}2.3$_WT (6), $K_{Ca}2.3$_G351D (7), and $K_{Ca}2.3$_I438N (5). Data are presented as mean ± SD. ***$P < 0.001$ compared with $K_{Ca}2.3$_WT.

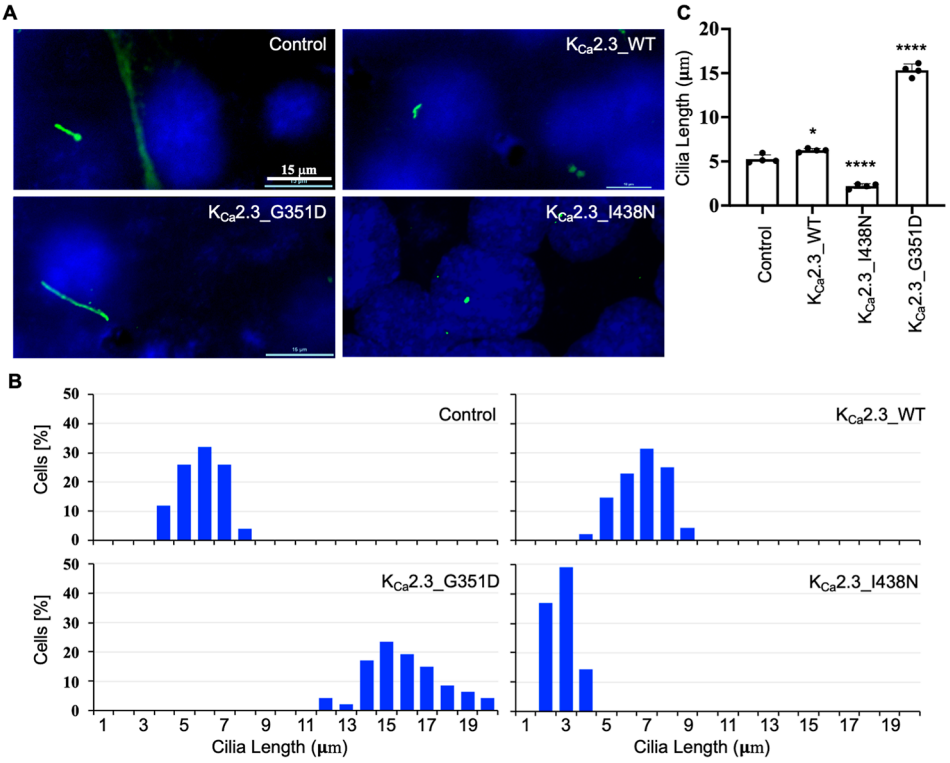

Figure 5. Expression of mouse $K_{Ca}2.3$ channels changes the primary cilia length in ET cells. (A) Cells were stained with the antibody of the ciliary marker acetylated α-tubulin (green) and the nuclear marker DAPI (blue). (B) Cilia length was grouped in a discreet range, and percent distribution was tabulated. (C) Cilia length is significantly longer in cells expressing $K_{Ca}2.3$_WT and $K_{Ca}2.3$_G351D but shorter in cells expressing $K_{Ca}2.3$_I438N channels. $N = 50-70$ for each slide preparation, and a total of four independent slides were used in each group. Data are presented as mean ± SD. *$p < 0.05$ and ****$p < 0.0001$ compared to the control.

cannot be used for the measurement of cilia length. Consistent with the measurements with acetylated α-tubulin (Figure 3), compound **4** (20 μM) increased cilia length (Figure S7B,C). A bee venom toxin, apamin (50 nM),[37] that selectively blocks $K_{Ca}2$ channels, completely abolished the elongating effect of compound **4** on cilia (Figure S7B,C). The ET cells do not express $K_{Ca}2.1$, $K_{Ca}2.2$, and $K_{Ca}3.1$ channels.[36] Therefore, the effect of apamin on the ET cells is mediated by the $K_{Ca}2.3$ channel blockade.

2.4. Expression of Mutant $K_{Ca}2.3$ Channels Affects Cilia Length. Positive modulators of $K_{Ca}2.3$ channels potentiate channel activity by increasing the apparent Ca^{2+} sensitivity of the channels,[38] whereas negative modulators decrease the apparent Ca^{2+} sensitivity of the channels.[39] To rule out the possibility that compound **4** and AP14145 affected cilia length through their off-target effects other than $K_{Ca}2.3$ channels, we heterologously expressed mutant $K_{Ca}2.3$ channels with altered apparent Ca^{2+} sensitivity (Figure 4). When expressed in ET cells, the $K_{Ca}2.3$ channels exhibited an apparent Ca^{2+} sensitivity of 0.67 ± 0.11 μM ($n = 6$). The G351D mutation significantly increased the apparent Ca^{2+} sensitivity to 0.16 ± 0.04 μM ($n = 7$), while the I438N mutation significantly reduced the apparent Ca^{2+} sensitivity to 1.8 ± 0.3 μM ($n = 5$, Figure 4). Immunoblots (Figures S8A–

https://doi.org/10.1021/acschembio.2c00469
ACS Chem. Biol. 2022, 17, 2344−2354

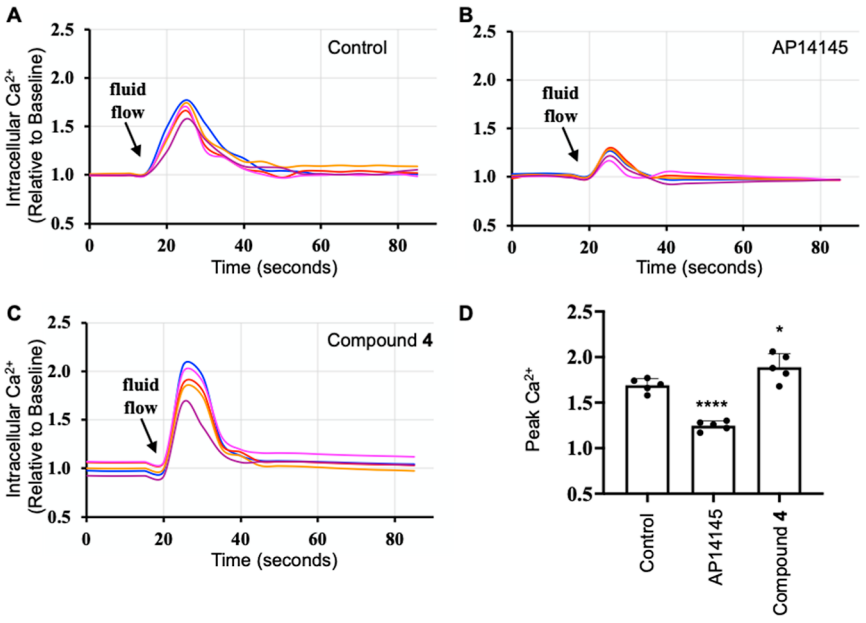

Figure 6. Positive and negative modulation of $K_{Ca}2.3$ channels affected flow-induced cytosolic Ca^{2+} signaling. Fluorescence Ca^{2+} measurements of ET cells treated with (A) solvent control, (B) negative modulator AP14145 (20 μM), and (C) positive modulator compound **4** (20 μM). (D) Peak Ca^{2+} values are significantly increased by compound **4** but reduced by AP14145. The numbers of independent measurements are shown in parentheses for the control (5), AP14145 (5), and compound **4** (5). Data are presented as mean ± SD. *p < 0.05 and ****p < 0.0001 compared with the control.

C) and immunostaining studies (Figure S8D) showed no evidence for different expression levels or localizations of the mutant channels.

The higher the apparent Ca^{2+} sensitivity of the mutant channel, the more likely the $K_{Ca}2.3$ channel is opening and then augmenting the Ca^{2+} influx in a positive feedback mechanism. The overexpression of $K_{Ca}2.3$_WT led to a slightly increased cilia length (6.3 ± 0.2 μm) compared with the control (5.3 ± 0.5 μm, Figure 5). $K_{Ca}2.3$_G351D mutant channels with hypersensitivity to Ca^{2+} increased the cilia length even more drastically (15.3 ± 0.7 μm), while the $K_{Ca}2.3$_I438N mutant channels with hyposensitivity to Ca^{2+} reduced the cilia length (2.2 ± 0.3 μm, Figure 5), confirming a role of the $K_{Ca}2.3$ channel in the regulation of cilia length.

2.5. Pharmacological Intervention of $K_{Ca}2.3$ Channels Affected Ca^{2+} Signaling. The opening of $K_{Ca}2.3$ channels induces hyperpolarization, which may increase the inward electrochemical gradient for Ca^{2+} and thus augment the Ca^{2+} influx. Next, we investigated whether the positive modulation or negative modulation of $K_{Ca}2.3$ channels affected the Ca^{2+} signaling, using fluorescence Ca^{2+} imaging (Figure 6). Flow-induced cytosolic Ca^{2+} transients were measured using a ratiometric, high-affinity intracellular Ca^{2+} indicator Fura-2AM. Compared with the control ET cells (Figure 6A), the AP14145-treated ET cells exhibited much weaker Ca^{2+} transients (Figure 6B). In contrast, the compound **4**-treated ET cells exhibited more prominent Ca^{2+} transients (Figure 6C) than the control cells. The significant effects of a negative modulator AP14145 and a positive modulator compound **4** on the flow-induced peak Ca^{2+} values (Figure 6D) suggest a link between the $K_{Ca}2.3$ channel opening and Ca^{2+} signaling, triggered by the shear stress. We have previously generated the non-ciliated IFT88 knockout (KO) mouse ET cells.[40] Using these cells, we further validate that flow-induced cytosolic Ca^{2+} transients were largely abolished in IFT88 KO ET cells, suggesting the essential role of cilia in flow-induced Ca^{2+} signaling (Figure S9).

3. DISCUSSION

Among the four channel subtypes encoded by the mammalian *KCNN* genes, $K_{Ca}2.3$ closely resembles the $K_{Ca}2.2$ channel subtype in pharmacology.[41] The human $K_{Ca}2.2a$ channel does not express as well as the rat $K_{Ca}2.2a$ channel, which prevented us from performing inside-out patch clamp experiments. Human and rat $K_{Ca}2.2a$ channels are highly homologous, with differences only in the distal cytoplasmic N- and C-termini. In the transmembrane domains and in the cytoplasmic gate including the HA/HB helices (highlighted in green), which CyPPA interacts with, the similarity is 100% (Figure S10). The prototype subtype-selective positive modulator, CyPPA achieved selectivity for $K_{Ca}2.2$ and $K_{Ca}2.3$ channels over $K_{Ca}2.1$ and $K_{Ca}3.1$ subtypes.[35] CyPPA is also ∼2.7 times more potent on human $K_{Ca}2.3$ than on rat $K_{Ca}2.2a$ channels (Table 1). In this study, we identified a positive modulator, compound **4**, that is ∼21-fold selective for human $K_{Ca}2.3$ over rat $K_{Ca}2.2a$ channels (Table 1). Compound **4** is largely inactive on human $K_{Ca}2.1$ and human $K_{Ca}3.1$ channels (Figure S2). The significance of this study is not limited to compound **4** itself with an EC_{50} of ∼0.3 μM and a modest subtype-selectivity for human $K_{Ca}2.3$ over rat $K_{Ca}2.2a$ channels. The subtype selectivity of compound **4** for human $K_{Ca}2.3$ over rat $K_{Ca}2.2a$ channels relies on an I-to-V discrepancy in the HA/HB helices between the two subtypes (Figures 2 and S4), which may offer an opportunity for the development of even more subtype-selective modulators.

The expression of $K_{Ca}2.3$ together with $K_{Ca}3.1$ channels on the plasma membrane of ET cells is well-documented.[3−5] $K_{Ca}2.3$ channels functionally couple with mechanosensitive and TRP Ca^{2+}-entry channels (e.g. PKD2[11] and TRPV4[31]). We observed a positive feedback effect of $K_{Ca}2.3$ channels on the

https://doi.org/10.1021/acschembio.2c00469
ACS Chem. Biol. 2022, 17, 2344−2354

flow-induced intracellular Ca^{2+} signaling through cilia (Figure 6). Most importantly, the positive feedback extends back to cilia themselves as the positive modulator compound 4 increased the cilia length (Figure 3), while the negative modulator AP14145 reduced the cilia length (Figure S6). These observations allow us to connect $K_{Ca}2.3$ channels and cilia, two crucial components in the flow-induced Ca^{2+} signaling in ET cells, with implications in vasodilation and blood pressure regulation.

The regulation of cilia length by $K_{Ca}2.3$ channel positive and negative modulators (Figures 3 and S6) has been corroborated by the effects on cilial length of the mutant $K_{Ca}2.3$ channels with altered apparent Ca^{2+} sensitivity (Figures 4 and 5). Expression of the Ca^{2+}-hypersensitive $K_{Ca}2.3$_G351D mutant channel increased the cilia length, while the Ca^{2+}-hyposensitive $K_{Ca}2.3$_I438N mutant channel reduced the cilia length (Figure 5). It is noteworthy that the mouse $K_{Ca}2.3$_G351D mutation used in our study is equivalent to the human $K_{Ca}2.3$_G350D mutation, which causes Zimmermann-Laband syndrome (ZLS).[42] It has been speculated that during human embryonic development, excessive hyperpolarization due to hypersensitivity to Ca^{2+} of the ZLS-related mutant $K_{Ca}2.3$ channels might result in exaggerated vasodilation in response to shear stress. This in turn might cause edema and vascular ruptures in critical phases of embryonic development, leading to distal digital hypoplasia with aplastic or hypoplastic nails and terminal phalanges.[42] Our results showed that the equivalent mouse $K_{Ca}2.3$_G351D mutation caused hypersensitivity to Ca^{2+} (Figure 4), which may contribute to vasodilation mediated by the endothelium-derived hyperpolarization.[8,43,44] Our finding here that the expression of $K_{Ca}2.3$_G351D mutant channels increased cilia length in ET cells (Figure 5) could also be translated into increased sensitivity and vasodilation in response to blood flow. Both of these two mechanisms might underlie the vasodilation and vascular rupture speculated in the embryonic development of ZLS patients, although further studies will be needed to elucidate the developmental biology.

We and other laboratories have previously reported that rapamycin increases cilia length in epithelial cells, resulting in the inhibition of cell proliferation.[45,46] On the other hand, rapamycin-induced cilia length increase correlates to an elevated response to fluid shear stress in ET cells.[47] The function of primary cilia as mechanosensory organelles depends on the length of cilia; lengthening primary cilia enhance cellular mechanosensitivity.[48,49] Dopamine, for example, also increases cilia length and function, resulting in enhanced cellular mechanosensitivity.[50] While dopamine specificity was a concern, drugs that improve sensory cilia function by elongating cilia length have been coined "ciliotherapy".[51] A more specific cilia-targeted therapy in ET cells has also been proposed to remedy hypertension.[52,53] We therefore are hopeful that subtype-selective positive modulators of KCa2.3 channels (e.g., compound **4**) would have a great potential to be a potential ciliotherapy.

4. EXPERIMENTAL SECTION

4.1. Materials. Materials are listed in Table 2.

4.2. Electrophysiology. The effect of compounds on the $K_{Ca}2.x$/$K_{Ca}3.1$ channels was investigated as previously described.[54,55] Briefly, the rat $K_{Ca}2.2a$, human $K_{Ca}2.1$, human $K_{Ca}2.3$, or human $K_{Ca}3.1$ channel cDNA constructs were either generated in-house or through molecular cloning services (Genscript, Piscataway, NJ, USA). These channel cDNAs in the pIRES2-AcGFP1 vector, along with calmodulin cDNA in the pcDNA3.1 + vector, at a ratio of 10:1 (ORF ratios), were transfected into cells using the calcium−phosphate method. K_{Ca} currents were recorded 1−2 days after transfection using an Axon200B amplifier (Molecular Devices, San Jose, CA) at room temperature. The resistance of the patch electrodes ranged from 3 to 5 MΩ. The pipette solution contained the following (in mM): 140 KCl, 10 Hepes (pH 7.4), and 1 $MgSO_4$. The bath solution containing (in mM) 140 KCl, 10 Hepes (pH 7.2), 1 EGTA, 0.1 Dibromo-BAPTA, and 1 HEDTA was mixed with Ca^{2+} to obtain the desired free Ca^{2+} concentrations, calculated using the software written by Chris Patton (https://somapp.ucdmc.ucdavis.edu/pharmacology/bers/maxchelator/webmaxc/webmaxcS.htm). The Ca^{2+} concentra-

Table 2

reagent or resources	source	identifier
	Chemicals	
CyPPA	Alomone Labs	C-110
NS13001	ChemShuttle	104258
compound **2k**	in-house synthesis[34]	N/A
compound **2l**	in-house synthesis[34]	N/A
compound **2m**	in-house synthesis[34]	N/A
compound **2n**	in-house synthesis[34]	N/A
compound **2o**	in-house synthesis[34]	N/A
compound **2p**	in-house synthesis[34]	N/A
compound **2q**	in-house synthesis[34]	N/A
compound **2r**	in-house synthesis[34]	N/A
compound **2s**	in-house synthesis[34]	N/A
compound **2t**	in-house synthesis[34]	N/A
compound **2u**	in-house synthesis[34]	N/A
compound **2v**	in-house synthesis[34]	N/A
compound **3a**	in-house synthesis[34]	N/A
compound **3b**	in-house synthesis[34]	N/A
compound **3c**	in-house synthesis[34]	N/A
compound **3d**	in-house synthesis[34]	N/A
compound **3e**	in-house synthesis[34]	N/A
compound **3f**	in-house synthesis[34]	N/A
compound **3g**	in-house synthesis[34]	N/A
compound **4**	in-house synthesis[34]	N/A
Fura2-AM	Thermo Fisher Scientific	F-1221
DAPI	Southern Biotech	0100-20
	Antibodies	
fluorescein secondary antibody	Vector Labs Burlingame	FI-2000
anti-acetylated α-tubulin	Sigma-Aldrich	T-7451
anti-GFP	Novus Biological	NB600-308SS
anti-GAPDH	Abcam	ab181602
anti-Arl13b	Proteintech	17711-1-AP
anti-γ-tubulin	Proteintech	15176-1-AP
	Experimental Models: Cell Lines	
Human: HEK293	ATCC	CRL-11268
Mouse: ET	in-house[26,27]	N/A
Mouse: IFT88 KO	in-house[40]	N/A
	Recombinant DNA	
pcDNA3.1(+)	Thermo Fisher Scientific	V79020
pIRES2-AcGFP1	Takara Bio	632435
	Software and Algorithms	
GraphPad Prism 9.0.2	GraphPad Software Inc.	RRID: SCR_002798
Clampfit 10.5	Molecular Devices	RRID: SCR_011323
pClamp 10.5	Molecular Devices	RRID: SCR_011323
Clustal Omega server	https://www.ebi.ac.uk/Tools/msa/clustalo/	RRID: SCR_001591

https://doi.org/10.1021/acschembio.2c00469
ACS Chem. Biol. 2022, 17, 2344−2354

tions were verified using a Ca^{2+} calibration buffer kit (Thermo Fisher Scientific). Briefly, a standard curve was generated using the Ca^{2+} buffers from the kit and a fluorescence Ca^{2+} indicator. Then, the Ca^{2+} concentrations of the bath solution were determined through interpolation on the standard curve.

High-resistance seals (>1 GΩ) were formed before inside-out patches were obtained. The seal resistance of inside-out patches was >1 GΩ, when the intracellular face was initially exposed to a zero-Ca^{2+} bath solution. Currents were recorded by repetitive 1-*s*-voltage ramps from −100 to +100 mV from a holding potential of 0 mV. The currents were filtered at 2 kHz and digitized at a sampling frequency of 10 kHz. At the end of the experiment, the integrity of the patch was examined by switching the bath solution back to the zero-Ca^{2+} buffer. Data from patches, which maintained the seal resistance (>1 GΩ) after solution changes, were used for further analysis.

To measure the effect of the positive modulators, the intracellular face was exposed to bath solutions with 0.15 μM Ca^{2+}. One minute after the switching of bath solutions, 10 sweeps with a 1 s interval were recorded at a series of concentrations of the compound in the presence of 0.15 μM Ca^{2+}. The maximal $K_{Ca}2.x/K_{Ca}3.1$ current in response to 10 μM Ca^{2+} was then recorded.

To measure the effect of the negative modulator Ap14145, the intracellular face was exposed to bath solutions with 0.5 μM Ca^{2+}. One minute after the switching of bath solutions, 10 sweeps with a 1 s interval were recorded at a series of concentrations of AP14145 in the presence of 0.5 μM Ca^{2+}.

4.3. Cilia Measurements. Cilia length was measured by direct immunofluorescence for the cilia marker with anti-acetylated α-tubulin or Arl13b staining. The cells were fixed for 10 min (4% paraformaldehyde/2% sucrose in PBS) and permeabilized for 5 min (10% Triton X-100). Acetylated α-tubulin (1:10,000 dilution, Sigma-Aldrich, St. Louis, MO) or Arl13b (1:50 dilution, Proteintech, Rosemont, IL) and fluorescein isothiocyanate-conjugated (1:1000 dilution, Vector Labs Burlingame, CA) antibodies were each incubated with the cells for 1 h at 37 °C. Microscope slides were then mounted with DAPI (Southern Biotech, Birmingham, AL) hard set mounting media. A Nikon Eclipse Ti-E inverted microscope with NIS-Elements imaging software (version 4.30) was used to capture the images of primary cilia. Automated image acquisition was conducted in 100× magnification fields. Cilia length analysis followed a standard calculation as previously described.[56]

4.4. Flow-Induced Ca^{2+} Measurements. Cells were loaded with 5 μM Fura2-AM (Thermo Fisher Scientific, Waltham, MA) at 37 °C for 30 min. Cells were then washed with Dulbecco's phosphate-buffered saline and observed under a 40× objective lens using a Nikon Eclipse Ti-E microscope controlled by Elements software. Cytosolic calcium was observed by recording Ca^{2+}-bound Fura excitation fluorescence at 340/380 nm and emission at 510 nm. Baseline Ca^{2+} was observed for 5 min prior to data acquisition. Fluid shear stress was then applied to cells utilizing an Instech P720 peristaltic pump with an inlet and outlet setup. The fluid was perfused on the glass-bottom plates at a shear stress of 5 dyn/cm^2. After each experiment, the maximum calcium signal was obtained with ATP (10 μM) to confirm cell viability. Conditions for all experiments were maintained at 37 °C and 5% CO_2 in a stage top cage incubator (okoLab, Burlingame, CA). Ca^{2+} analysis followed a standard calculation as previously described.[56]

4.5. Immunoblots. The protein concentrations in ET cell lysates were determined using a BCA protein assay kit (Thermo Fisher Scientific, Waltham, MA). Equal amounts of protein (15 μg) were separated by sodium dodecyl sulfate−polyacrylamide gel electrophoresis gel (Bio-Rad Laboratories, Hercules, CA). The proteins were transferred to polyvinylidene fluoride (PVDF) membranes and incubated overnight at 4 °C with the primary GFP antibody (1:2000; Novus Biological, Centennial, CO) or GAPDH antibody (1:5000; Abcam, Waltham, MA). The PVDF membranes were washed with Tris-buffered saline (0.1% Tween 20) and incubated with the anti-rabbit antibody (1:3000; cell signaling technology, Danvers, MA) as the secondary antibody for 1 h at room temperature and then washed with Tris-buffered saline (0.1% Tween 20). The chemiluminescence signals were detected on a ChemiDoc XRS system (Bio-Rad Laboratories, Hercules, CA) after incubation with Luminol/enhancer solution (Thermo Fisher Scientific, Waltham, MA). Densitometry analyses were performed using the ImageJ computer program.

4.6. Data and Statistical Analysis. Patch clamp recordings were analyzed using Clampfit 10.5 (Molecular Devices LLC, San Jose, CA), and concentration−response curves were analyzed in GraphPad Prism 9.0.2 (GraphPad Software Inc., La Jolla, CA). To construct the concentration-dependent potentiation of channel activities by the compound, the current amplitudes at −90 mV in response to various concentrations of the compound were normalized to that obtained at a maximal concentration of the compound. The normalized currents were plotted as a function of the concentrations of the compound. EC_{50} values and Hill coefficients were determined by fitting the data points to a standard concentration−response curve $[Y = 100/(1 + (X/EC50)^{\wedge} - \text{Hill})]$. To assess the efficacy of the compound, the current amplitudes obtained at the maximal concentration of the compound were normalized to the maximal $K_{Ca}2.x/K_{Ca}3.1$ current in response to 10 μM Ca^{2+}. Concentration−response curves were acquired from multiple patches for each data set. Each curve was fitted individually, which yielded the EC_{50} value for that curve. EC_{50} values are shown as mean ± SD obtained from multiple patches, and the number of patches is indicated by *n*.

The Student's *t*-test was used for data comparison if there were only two groups. One-way ANOVA and Tukey's post hoc tests were used for data comparison of three or more groups. Post hoc tests were carried out only if *F* was significant and there was no variance in homogeneity.

■ ASSOCIATED CONTENT

Supporting Information

The Supporting Information is available free of charge at https://pubs.acs.org/doi/10.1021/acschembio.2c00469.

Electrophysiological recordings, cilia length measurements, intracellular Ca^{2+} signaling data, and amino acid sequence alignments (PDF)

■ AUTHOR INFORMATION

Corresponding Authors

Surya M. Nauli − *Department of Biomedical and Pharmaceutical Sciences, Chapman University School of Pharmacy, Irvine, California 92618, USA;* orcid.org/0000-0002-9676-0287; Phone: +1-714-516-5485; Email: nauli@chapman.edu; Fax: +1-714-516-5481

Miao Zhang − *Department of Biomedical and Pharmaceutical Sciences, Chapman University School of Pharmacy, Irvine, California 92618, USA;* orcid.org/0000-0002-3099-155X; Phone: +1-714-516-5478; Email: zhang@chapman.edu; Fax: +1-714-516-5481

Authors

Young-Woo Nam − *Department of Biomedical and Pharmaceutical Sciences, Chapman University School of Pharmacy, Irvine, California 92618, USA*

Rajasekharreddy Pala − *Department of Biomedical and Pharmaceutical Sciences, Chapman University School of Pharmacy, Irvine, California 92618, USA;* orcid.org/0000-0001-9787-1053

Naglaa Salem El-Sayed − *Department of Biomedical and Pharmaceutical Sciences, Chapman University School of Pharmacy, Irvine, California 92618, USA;* Present Address: Cellulose and Paper Department, National Research Center, 33 El-Bouhos St. (former Tahrir St.), Dokki, Giza, Egypt, P.O.X 12622

https://doi.org/10.1021/acschembio.2c00469
ACS Chem. Biol. 2022, 17, 2344−2354

Denisse Larin-Henriquez − *Department of Biomedical and Pharmaceutical Sciences, Chapman University School of Pharmacy, Irvine, California 92618, USA*
Farideh Amirrad − *Department of Biomedical and Pharmaceutical Sciences, Chapman University School of Pharmacy, Irvine, California 92618, USA*
Grace Yang − *Department of Biomedical and Pharmaceutical Sciences, Chapman University School of Pharmacy, Irvine, California 92618, USA*
Mohammad Asikur Rahman − *Department of Biomedical and Pharmaceutical Sciences, Chapman University School of Pharmacy, Irvine, California 92618, USA*
Razan Orfali − *Department of Biomedical and Pharmaceutical Sciences, Chapman University School of Pharmacy, Irvine, California 92618, USA*
Myles Downey − *Department of Biomedical and Pharmaceutical Sciences, Chapman University School of Pharmacy, Irvine, California 92618, USA*
Keykavous Parang − *Department of Biomedical and Pharmaceutical Sciences, Chapman University School of Pharmacy, Irvine, California 92618, USA;* orcid.org/0000-0001-8600-0893

Complete contact information is available at: https://pubs.acs.org/10.1021/acschembio.2c00469

Author Contributions

Y.-W.N. and P.R. contributed equally to this work. Y.W.N., G.Y., R.O., M.A.R, M.D., and M.Z. undertook molecular biology and in vitro electrophysiology studies. P.R., D.L-H., F.A., and S.M.N. undertook cilia and Ca^{2+} imaging studies. N.S.E. and K.P. undertook chemical synthesis. S.M.N. and M.Z. wrote the manuscript. All authors contributed to the figures. All authors have read and agreed to the published version of the manuscript.

Funding

M.Z. was supported by an Internal Faculty Opportunity Fund of Chapman University Office of Research, a Scientist Development grant 13SDG16150007 from American Heart Association, and a National Institutes of Health grant 4R33NS101182. S.M.N. was supported by a National Institutes of Health grant R01HL147311.

Notes

The authors declare no competing financial interest.

■ ACKNOWLEDGMENTS

We are grateful to L.Basilio, Y.Hur, and M.Nguyen for technical assistance.

■ ABBREVIATIONS

$K_{Ca}2.1$ channels, small-conductance Ca^{2+}-activated potassium subtype 1 channels; $K_{Ca}2.2$ channels, small-conductance Ca^{2+}-activated potassium subtype 2 channels; $K_{Ca}2.3$ channels, small-conductance Ca^{2+}-activated potassium subtype 3 channels; $K_{Ca}3.1$ channels, intermediate-conductance Ca^{2+}-activated potassium channels; Ca_v, voltage-gated Ca^{2+} channels; ER, endoplasmic reticulum; TRP, transient receptor potential; NO, nitric oxide; PKD2, polycystic kidney disease; ZLS, Zimmermann-Laband syndrome

■ REFERENCES

(1) Adelman, J. P.; Maylie, J.; Sah, P. Small-conductance Ca2+-activated K+ channels: form and function. *Annu. Rev. Physiol.* **2012**, *74*, 245−269.
(2) Brown, B. M.; Shim, H.; Christophersen, P.; Wulff, H. Pharmacology of small- and intermediate-conductance calcium-activated potassium channels. *Annu. Rev. Pharmacol. Toxicol.* **2020**, *60*, 219−240.
(3) Liu, Y.; Xie, A.; Singh, A. K.; Ehsan, A.; Choudhary, G.; Dudley, S.; Sellke, F. W.; Feng, J. Inactivation of Endothelial Small/Intermediate Conductance of Calcium-Activated Potassium Channels Contributes to Coronary Arteriolar Dysfunction in Diabetic Patients. *J. Am. Heart Assoc.* **2015**, *4*, No. e002062.
(4) Köhler, R.; Brakemeier, S.; Kühn, M.; Behrens, C.; Real, R.; Degenhardt, C.; Orzechowski, H. D.; Pries, A. R.; Paul, M.; Hoyer, J. Impaired hyperpolarization in regenerated endothelium after balloon catheter injury. *Circ. Res.* **2001**, *89*, 174.
(5) Köhler, R.; Degenhardt, C.; Kühn, M.; Runkel, N.; Paul, M.; Hoyer, J. Expression and function of endothelial Ca(2+)-activated K(+) channels in human mesenteric artery: A single-cell reverse transcriptase-polymerase chain reaction and electrophysiological study in situ. *Circ. Res.* **2000**, *87*, 496−503.
(6) Wulff, H.; Köhler, R. Endothelial small-conductance and intermediate-conductance KCa channels: an update on their pharmacology and usefulness as cardiovascular targets. *J. Cardiovasc. Pharmacol.* **2013**, *61*, 102−112.
(7) Ledoux, J.; Taylor, M. S.; Bonev, A. D.; Hannah, R. M.; Solodushko, V.; Shui, B.; Tallini, Y.; Kotlikoff, M. I.; Nelson, M. T. Functional architecture of inositol 1,4,5-trisphosphate signaling in restricted spaces of myoendothelial projections. *Proc. Natl. Acad. Sci. U. S. A.* **2008**, *105*, 9627−9632.
(8) Dora, K. A.; Gallagher, N. T.; McNeish, A.; Garland, C. J. Modulation of endothelial cell KCa3.1 channels during endothelium-derived hyperpolarizing factor signaling in mesenteric resistance arteries. *Circ. Res.* **2008**, *102*, 1247−1255.
(9) Sandow, S. L.; Neylon, C. B.; Chen, M. X.; Garland, C. J. Spatial separation of endothelial small- and intermediate-conductance calcium-activated potassium channels (K(Ca)) and connexins: possible relationship to vasodilator function? *J. Anat.* **2006**, *209*, 689−698.
(10) Brähler, S.; Kaistha, A.; Schmidt, V. J.; Wölfle, S. E.; Busch, C.; Kaistha, B. P.; Kacik, M.; Hasenau, A. L.; Grgic, I.; Si, H.; et al. Genetic deficit of SK3 and IK1 channels disrupts the endothelium-derived hyperpolarizing factor vasodilator pathway and causes hypertension. *Circulation* **2009**, *119*, 2323.
(11) MacKay, C. E.; Leo, M. D.; Fernandez-Pena, C.; Hasan, R.; Yin, W.; Mata-Daboin, A.; Bulley, S.; Gammons, J.; Mancarella, S.; Jaggar, J. H. Intravascular flow stimulates PKD2 (polycystin-2) channels in endothelial cells to reduce blood pressure. *Elife* **2020**, *9*, No. e60401.
(12) Sheng, J. Z.; Ella, S.; Davis, M. J.; Hill, M. A.; Braun, A. P. Openers of SKCa and IKCa channels enhance agonist-evoked endothelial nitric oxide synthesis and arteriolar vasodilation. *FASEB J.* **2009**, *23*, 1138−1145.
(13) Stankevicius, E.; Lopez-Valverde, V.; Rivera, L.; Hughes, A. D.; Mulvany, M. J.; Simonsen, U. Combination of Ca2+ -activated K+ channel blockers inhibits acetylcholine-evoked nitric oxide release in rat superior mesenteric artery. *Br. J. Pharmacol.* **2006**, *149*, 560−72.
(14) Saternos, H. C.; AbouAlaiwi, W. A. Implications of Dysfunction of Mechanosensory Cilia in Polycystic Kidney Disease. In *Polycystic Kidney Disease*; Li, X., Ed.; Exon Publications: Brisbane (AU), 2015.
(15) Phua, S. C.; Lin, Y. C.; Inoue, T. An intelligent nano-antenna: Primary cilium harnesses TRP channels to decode polymodal stimuli. *Cell Calcium* **2015**, *58*, 415−422.
(16) Ando, J.; Yamamoto, K. Flow detection and calcium signalling in vascular endothelial cells. *Cardiovasc. Res.* **2013**, *99*, 260−268.
(17) Cortellino, S.; Wang, C.; Wang, B.; Bassi, M. R.; Caretti, E.; Champeval, D.; Calmont, A.; Jarnik, M.; Burch, J.; Zaret, K. S.; et al. Defective ciliogenesis, embryonic lethality and severe impairment of the Sonic Hedgehog pathway caused by inactivation of the mouse

complex A intraflagellar transport gene Ift122/Wdr10, partially overlapping with the DNA repair gene Med1/Mbd4. *Dev. Biol.* **2009**, *325*, 225−237.
(18) Wu, G.; Markowitz, G. S.; Li, L.; D'Agati, V. D.; Factor, S. M.; Geng, L.; Tibara, S.; Tuchman, J.; Cai, Y.; Hoon Park, J. H.; et al. Cardiac defects and renal failure in mice with targeted mutations in Pkd2. *Nat. Genet.* **2000**, *24*, 75−78.
(19) Lu, W.; Peissel, B.; Babakhanlou, H.; Pavlova, A.; Geng, L.; Fan, X.; Larson, C.; Brent, G.; Zhou, J. Perinatal lethality with kidney and pancreas defects in mice with a targetted Pkd1 mutation. *Nat. Genet.* **1997**, *17*, 179−181.
(20) Yoder, B. K.; Richards, W. G.; Sweeney, W. E.; Wilkinson, J. E.; Avener, E. D.; Woychik, R. P. Insertional mutagenesis and molecular analysis of a new gene associated with polycystic kidney disease. *Proc. Assoc. Am. Physicians* **1995**, *107*, 314.
(21) Mohieldin, A. M.; Zubayer, H. S.; Al Omran, A. J.; Saternos, H. C.; Zarban, A. A.; Nauli, S. M.; AbouAlaiwi, W. A. Vascular Endothelial Primary Cilia: Mechanosensation and Hypertension. *Curr. Hypertens. Rev.* **2016**, *12*, 57−67.
(22) Luo, N.; Conwell, M. D.; Chen, X.; Kettenhofen, C. I.; Westlake, C. J.; Cantor, L. B.; Wells, C. D.; Weinreb, R. N.; Corson, T. W.; Spandau, D. F.; et al. Primary cilia signaling mediates intraocular pressure sensation. *Proc. Natl. Acad. Sci. U. S. A.* **2014**, *111*, 12871−12876.
(23) Nguyen, A. M.; Jacobs, C. R. Emerging role of primary cilia as mechanosensors in osteocytes. *Bone* **2013**, *54*, 196−204.
(24) Praetorius, H. A.; Spring, K. R. Removal of the MDCK cell primary cilium abolishes flow sensing. *J. Membr. Biol.* **2003**, *191*, 69−76.
(25) Schwartz, E. A.; Leonard, M. L.; Bizios, R.; Bowser, S. S. Analysis and modeling of the primary cilium bending response to fluid shear. *Am. J. Physiol.* **1997**, *272*, F132.
(26) AbouAlaiwi, W. A.; Takahashi, M.; Mell, B. R.; Jones, T. J.; Ratnam, S.; Kolb, R. J.; Nauli, S. M. Ciliary polycystin-2 is a mechanosensitive calcium channel involved in nitric oxide signaling cascades. *Circ. Res.* **2009**, *104*, 860−869.
(27) Nauli, S. M.; Kawanabe, Y.; Kaminski, J. J.; Pearce, W. J.; Ingber, D. E.; Zhou, J. Endothelial cilia are fluid shear sensors that regulate calcium signaling and nitric oxide production through polycystin-1. *Circulation* **2008**, *117*, 1161−1171.
(28) Pablo, J. L.; DeCaen, P. G.; Clapham, D. E. Progress in ciliary ion channel physiology. *J. Gen. Physiol.* **2017**, *149*, 37−47.
(29) Nauli, S. M.; Pala, R.; Kleene, S. J. Calcium channels in primary cilia. *Curr. Opin. Nephrol. Hypertens.* **2016**, *25*, 452−458.
(30) Gerhold, K. A.; Schwartz, M. A. Ion Channels in Endothelial Responses to Fluid Shear Stress. *Physiol.* **2016**, *31*, 359−369.
(31) Sonkusare, S. K.; Bonev, A. D.; Ledoux, J.; Liedtke, W.; Kotlikoff, M. I.; Heppner, T. J.; Hill-Eubanks, D. C.; Nelson, M. T. Elementary Ca2+ signals through endothelial TRPV4 channels regulate vascular function. *Science* **2012**, *336*, 597−601.
(32) Qian, X.; Francis, M.; Köhler, R.; Solodushko, V.; Lin, M.; Taylor, M. S. Positive feedback regulation of agonist-stimulated endothelial Ca2+ dynamics by KCa3.1 channels in mouse mesenteric arteries. *Arterioscler., Thromb., Vasc. Biol.* **2014**, *34*, 127−135.
(33) Nam, Y. W.; Cui, M.; Salem, N.; Orfali, R.; Nguyen, M.; Yang, G.; Rahman, M. A.; Lee, J.; Zhang, M. Subtype-selective positive modulation of KCa 2 channels depends on the HA/HB helices. *Br. J. Pharmacol.* **2021**, *179*, 460.
(34) El-Sayed, N. S.; Nam, Y. W.; Egorova, P. A.; Nguyen, H. M.; Orfali, R.; Rahman, M. A.; Yang, G.; Wulff, H.; Bezprozvanny, I.; Parang, K.; et al. Structure-Activity Relationship Study of Subtype-Selective Positive Modulators of KCa2 Channels. *J. Med. Chem.* **2021**, *65*, 303.
(35) Hougaard, C.; Eriksen, B. L.; Jørgensen, S.; Johansen, T. H.; Dyhring, T.; Madsen, L. S.; Strøbaek, D.; Christophersen, P. Selective positive modulation of the SK3 and SK2 subtypes of small conductance Ca2+-activated K+ channels. *Br. J. Pharmacol.* **2007**, *151*, 655−665.
(36) Nam, Y. W.; Kong, D.; Wang, D.; Orfali, R.; Sherpa, R. T.; Totonchy, J.; Nauli, S. M.; Zhang, M. Differential modulation of SK channel subtypes by phosphorylation. *Cell Calcium* **2021**, *94*, 102346.
(37) Lamy, C.; Goodchild, S. J.; Weatherall, K. L.; Jane, D. E.; Liégeois, J. F.; Seutin, V.; Marrion, N. V. Allosteric block of KCa2 channels by apamin. *J. Biol. Chem.* **2010**, *285*, 27067−27077.
(38) Hougaard, C.; Eriksen, B. L.; Jørgensen, S.; Johansen, T. H.; Dyhring, T.; Madsen, L. S.; Strøbaek, D.; Christophersen, P. Selective positive modulation of the SK3 and SK2 subtypes of small conductance Ca2+-activated K+ channels. *Br. J. Pharmacol.* **2007**, *151*, 655−665.
(39) Simó-Vicens, R.; Kirchhoff, J. E.; Dolce, B.; Abildgaard, L.; Speerschneider, T.; Sørensen, U. S.; Grunnet, M.; Diness, J. G.; Bentzen, B. H. A new negative allosteric modulator, AP14145, for the study of small conductance calcium-activated potassium (KCa 2) channels. *Br. J. Pharmacol.* **2017**, *174*, 4396−4408.
(40) Mohieldin, A. M.; Pala, R.; Beuttler, R.; Moresco, J. J.; Yates, J. R., 3rd; Nauli, S. M. Ciliary extracellular vesicles are distinct from the cytosolic extracellular vesicles. *J. Extracell. Vesicles* **2021**, *10*, No. e12086.
(41) Aldrich, R. W.; Chandy, K. G.; Grissmer, S.; Gutman, G. A.; Kaczmarek, L. K.; Wei, A. D.; Wulff, H. *Calcium- and Sodium-Activated Potassium Channels (Version 2019.4) in the IUPHAR/BPS Guide to Pharmacology Database*; IUPHAR/BPS Guide to Pharmacology CITE, 2019.
(42) Bauer, C. K.; Schneeberger, P. E.; Kortüm, F.; Altmüller, J.; Santos-Simarro, F.; Baker, L.; Keller-Ramey, J.; White, S. M.; Campeau, P. M.; Gripp, K. W.; et al. Gain-of-Function Mutations in KCNN3 Encoding the Small-Conductance Ca(2+)-Activated K(+) Channel SK3 Cause Zimmermann-Laband Syndrome. *Am. J. Hum. Genet.* **2019**, *104*, 1139−1157.
(43) Marrelli, S. P.; Eckmann, M. S.; Hunte, M. S. Role of endothelial intermediate conductance KCa channels in cerebral EDHF-mediated dilations. *Am. J. Physiol.* **2003**, *285*, H1590−H1599.
(44) Edwards, G.; Félétou, M.; Weston, A. H. Endothelium-derived hyperpolarising factors and associated pathways: a synopsis. *Pfluegers Arch. Eur. J. Physiol.* **2010**, *459*, 863−879.
(45) Jamal, M. H.; Nunes, A. C. F.; Vaziri, N. D.; Ramchandran, R.; Bacallao, R. L.; Nauli, A. M.; Nauli, S. M. Rapamycin treatment correlates changes in primary cilia expression with cell cycle regulation in epithelial cells. *Biochem. Pharmacol.* **2020**, *178*, 114056.
(46) Khan, N. A.; Willemarck, N.; Talebi, A.; Marchand, A.; Binda, M. M.; Dehairs, J.; Rueda-Rincon, N.; Daniels, V. W.; Bagadi, M.; Raj, D. B.; et al. Identification of drugs that restore primary cilium expression in cancer cells. *Oncotarget* **2016**, *7*, 9975−9992.
(47) Sherpa, R. T.; Atkinson, K. F.; Ferreira, V. P.; Nauli, S. M. Rapamycin Increases Length and Mechanosensory Function of Primary Cilia in Renal Epithelial and Vascular Endothelial Cells. *Int. J. Educ. Res.* **2016**, *2*, 91−97.
(48) Upadhyay, V. S.; Muntean, B. S.; Kathem, S. H.; Hwang, J. J.; AbouAlaiwi, W. A.; Nauli, S. M. Roles of dopamine receptor on chemosensory and mechanosensory primary cilia in renal epithelial cells. *Front. Physiol.* **2014**, *5*, 72.
(49) Spasic, M.; Jacobs, C. R.; Jacobs, C. Lengthening primary cilia enhances cellular mechanosensitivity. *Eur. Cells Mater.* **2017**, *33*, 158−168.
(50) Abdul-Majeed, S.; Nauli, S. M. Dopamine receptor type 5 in the primary cilia has dual chemo- and mechano-sensory roles. *Hypertension* **2011**, *58*, 325−331.
(51) Kathem, S. H.; Mohieldin, A. M.; Abdul-Majeed, S.; Ismail, S. H.; Altaei, Q. H.; Alshimmari, I. K.; Alsaidi, M. M.; Khammas, H.; Nauli, A. M.; Joe, B.; et al. Ciliotherapy: a novel intervention in polycystic kidney disease. *J. Geriatr. Cardiol.* **2014**, *11*, 63−73.
(52) Pala, R.; Mohieldin, A. M.; Sherpa, R. T.; Kathem, S. H.; Shamloo, K.; Luan, Z.; Zhou, J.; Zheng, J. G.; Ahsan, A.; Nauli, S. M. Ciliotherapy: Remote Control of Primary Cilia Movement and Function by Magnetic Nanoparticles. *ACS Nano* **2019**, *13*, 3555−3572.

https://doi.org/10.1021/acschembio.2c00469
ACS Chem. Biol. 2022, 17, 2344−2354

(53) Pala, R.; Mohieldin, A. M.; Shamloo, K.; Sherpa, R. T.; Kathem, S. H.; Zhou, J.; Luan, Z.; Zheng, J. G.; Ahsan, A.; Nauli, S. M. Personalized Nanotherapy by Specifically Targeting Cell Organelles To Improve Vascular Hypertension. *Nano Lett.* **2019**, *19*, 904−914.
(54) Nam, Y. W.; Baskoylu, S. N.; Gazgalis, D.; Orfali, R.; Cui, M.; Hart, A. C.; Zhang, M. A V-to-F substitution in SK2 channels causes Ca(2+) hypersensitivity and improves locomotion in a C. elegans ALS model. *Sci. Rep.* **2018**, *8*, 10749.
(55) Nam, Y. W.; Cui, M.; Orfali, R.; Viegas, A.; Nguyen, M.; Mohammed, E. H. M.; Zoghebi, K. A.; Rahighi, S.; Parang, K.; Zhang, M. Hydrophobic interactions between the HA helix and S4-S5 linker modulate apparent Ca(2+) sensitivity of SK2 channels. *Acta Physiol.* **2021**, *231*, No. e13552.
(56) Nauli, S. M.; Jin, X.; AbouAlaiwi, W. A.; El-Jouni, W.; Su, X.; Zhou, J. Non-motile primary cilia as fluid shear stress mechanosensors. *Methods Enzymol.* **2013**, *525*, 1−20.

https://doi.org/10.1021/acschembio.2c00469
ACS Chem. Biol. 2022, 17, 2344−2354